System–Dependent Signatures of Electronic and Vibrational Coherences in Electronic 2D–Spectra

7 AUTHORS, INCLUDING:

Tomas Mancal
Charles University in Prague
66 PUBLICATIONS   **2,784** CITATIONS

SEE PROFILE

Franz Milota
JTI R&D
51 PUBLICATIONS   **902** CITATIONS

SEE PROFILE

Oliver Bixner
Nanyang Technological University
6 PUBLICATIONS   **192** CITATIONS

SEE PROFILE

Jürgen Hauer
TU Wien
51 PUBLICATIONS   **800** CITATIONS

SEE PROFILE

System-Dependent Signatures of Electronic and Vibrational Coherences in Electronic Two-Dimensional Spectra

Tomáš Mančal,[†] Niklas Christensson,[‡] Vladimír Lukeš,[§] Franz Milota,[‡] Oliver Bixner,[‡] Harald F. Kauffmann,[‡,||] and Jürgen Hauer*[,‡]

[†]Institute of Physics, Faculty of Mathematics and Physics, Charles University, Ke Karlovu 5, Prague 121 16, Czech Republic
[‡]Faculty of Physics, University of Vienna, Strudlhofgasse 4, 1090 Vienna, Austria
[§]Department of Chemical Physics, Slovak Technical University, Radlinského 9, 81237 Bratislava, Slovakia
[||]Faculty of Physics, Vienna University of Technology, Wiedner Hauptstrasse 8 - 10, 1040 Vienna, Austria

Ⓢ *Supporting Information*

ABSTRACT: In this work, we examine vibrational coherence in a molecular monomer, where time evolution of a nuclear wavepacket gives rise to oscillating diagonal- and off-diagonal peaks in two-dimensional electronic spectra. We find that the peaks oscillate out-of-phase, resulting in a cancellation in the corresponding pump–probe spectra. Our results confirm the unique disposition of two-dimensional electronic spectroscopy (2D-ES) for the study of coherences. The oscillation pattern is in excellent agreement with the diagrammatic analysis of the third-order nonlinear response. We show how 2D-ES can be used to distinguish between ground- and excited-state wavepackets. On the basis of our results, we discuss coherences in coupled molecular aggregates involving both electronic and nuclear degrees of freedom. We conclude that a general distinguishing criterion based on the experimental data alone cannot be devised.
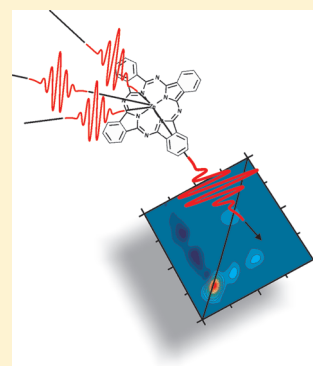
SECTION: Spectroscopy, Photochemistry, and Excited States

Since the advent of ultrashort laser pulses three decades ago, spectroscopy utilizing sequences of short laser pulses has opened a unique window into the properties of molecular systems on ultrafast time scales. From the quantum mechanical perspective, most molecular systems can be reduced to certain simple discrete level structures. Many properties of such multilevel systems do not depend on their exact nature, e.g., vibrational or electronic. One common feature is the possibility to excite a coherent superposition of energy eigenstates,[1] i.e., a quantum mechanical wavepacket. Despite their similarities, electronic and vibrational coherence reflect distinctly different physics. Vibrational coherence is typically associated with a single chromophore,[2,3] while electronic coherence in a molecular aggregate may stem from collective effects involving multiple pigments.[4,5] The different nature of the energy levels is also reflected in the dephasing dynamics of the associated coherence. The electronic degrees of freedom (DOFs) couple to a macroscopic number of vibrational DOFs, and the electronic coherence is therefore expected to undergo rapid dephasing. The vibrational DOFs, on the other hand, may be understood as a result of normal-mode analysis, and are in first approximation decoupled from all other modes. As a result, vibrational coherence is expected to display dephasing times at least an order of magnitude longer than those expected for the purely electronic coherence.

Recently, the problem of the photoinduced coherence observed in two-dimensional electronic spectra (2D-ES) of light harvesting complexes[4,5] has attracted a lot of attention. It was suggested that the observed coherence originates from a superposition of electronic eigenstates, and that its long lifetime is of central importance for the high efficiency of light harvesting systems.[4] The analysis by Cheng and Fleming[6] showed that electronic coherence beatings in an electronic dimer lead to an oscillating diagonal peak in the nonrephasing spectrum, while the corresponding rephasing peak is static. Turner et al.[3,7] have applied this argument on experimental data in order to distinguish between electronic and vibrational coherence. However, when electronic and vibrational DOFs are simultaneously present in a coupled system, the energy levels in the excited state acquire a mixed character.[8] The excited state energy level structure will then be similar to the electronic case, but certain levels may possess a significant vibrational character.[9,10]

Therefore, it is unclear to what extent one can find experimental signatures enabling an unbiased determination of the nature of an observed coherence. In this work we examine zinc-phthalocyanine (ZnPc), a solvated monomer, with 2D-ES in order to identify features unique to vibrational coherences. We explicitly include vibrational levels in a

discussion of individual Liouville pathways in third-order nonlinear response. This analysis readily explains how specific peaks oscillate out of phase, resulting in cancellation in pump–probe spectra. On the basis of the derived model, we conclude by discussing the feasibility of distinguishing electronic and vibrational coherences in a realistic molecular aggregate.

Experimental Results. Our experimental layout for 2D-ES was described before.[11] Details of the employed calibration procedures for time and frequency axes are given in the Supporting Information. 2D-ES experiments were carried out using sub-8 fs noncollinear parametric amplification (NOPA) pulses centered at 15 000 cm^{-1} (670 nm), as shown in Figure 1A. ZnPc was dissolved in benzonitrile, and the concentration was set to obtain an optical density of 0.13 OD for a layer thickness of 180 μm in a flowing sample jet.[11] The employed phase matching direction was $k_S = -k_1 + k_2 + k_3$. The time-

ordering of the conjugate field along $-k_1$ defines the experimental signals: Time orders 1−2−3 and 2−1−3 correspond to rephasing and nonrephasing signals, respectively, with the total signal, $S^{2D}(\omega_1, t_2, \omega_3)$, as their sum. At a given population time t_2 (the delay between the second and third pulses), the signal is measured as a function of t_1, the delay between the first two pulses, and the detection frequency ω_3. Applying the Fourier-transformation along t_1 and a phasing procedure described in the literature,[12] we obtain $S^{2D}(\omega_1, t_2, \omega_3)$, whose real part can be interpreted as a 2D-correlation plot of the absorption and emission events separated by time delay t_2.

Figure 1A shows the real part of the electronic 2D spectrum of ZnPc at $t_2 = 143$ fs. As can be seen in the lower panel in Figure 1A, there is a weak but discernible vibrational progression besides the main Q-band.[13] The strongest feature in the 2D-spectrum lies on the diagonal ($\omega_1 = \omega_3$) and is readily identified as the Q-band's ground-state bleach (GSB), along with features from stimulated emission (SE) pathways. The spectral profile of the excited-state-absorption feature (ESA, blue lines) is broad and blue-shifted from the GSB-transition.[14] The two positive off-diagonal peaks are found at roughly the same detection frequency ω_3 as the main diagonal peak, and they are detuned by approximately 700 and 1600 cm^{-1} from it in ω_1. These detunings correspond to the vibrational progression peaks in the absorption spectrum. Therefore, the positive cross peaks in Figure 1A are assigned to vibrational levels.[2,15,16] We conducted a quantum chemical analysis using the (TD)-B3LYP/SV(P) functional to establish that both the 700 and the 1600 cm^{-1} mode are totally symmetric, and have Huang–Rhys factors of 0.112 and 0.214, respectively.[17] The vibrational spacing of roughly 700 cm^{-1} also motivates the choice of $t_2 = 143$ fs, as it corresponds to 3 times the vibrational period of the observed mode. The dotted horizontal line "line 0" in Figure 1A marks the detection frequency of the diagonal peak DP1 and the cross peak CP21. Lines $\pm$v are detuned by 700 cm^{-1} to higher (+v) and lower (−v) values of ω_3.

Figure 1B shows transients in t_2 for DP1 (black) and CP21 (red) as indicated in Figure 1A. Both shown transients are normalized to their respective mean values and correspond to the temporal development of single points on the 2D-spectrum. The same oscillatory behavior was observed when integrating an area of up to 50 × 50 cm^{-1}. To avoid pulse overlap effects, we start at 12 fs. The peak amplitudes show a modulation corresponding to the vibrational period of the 700 cm^{-1} ring-breathing mode of ZnPc. Interestingly, the transients for CP21 and DP1 oscillate out of phase, while the amplitudes of CP12 and DP2 oscillate in phase.

Diagrammatic Analysis of 2D Spectra. The relative phases of the oscillations in the different peaks can be understood via a diagrammatic treatment of the vibronic response first used by Farrow et al.[18] Figure 2 shows oscillatory GSB and SE pathways of DP1 and CP21 (line 0). ESA pathways are neglected in the rest of this work based on their blueshift (see Figure 1A).[14] Concerning solvent contribution to individual pathways, they are assumed to contribute as a prefactor, which is the same for all pathways of the same type (rephasing, nonrephasing).[16]

ZnPc is a square-symmetric (D_{4h}) molecule with two degenerate excited states, α and β, showing orthogonal transition dipole moments. Each electronic state has one vibrational level (ν'' or $\nu_{\alpha,\beta}'$). The full, dashed and wavy arrows in Figure 2 denote bra- or ket-interactions of the molecular
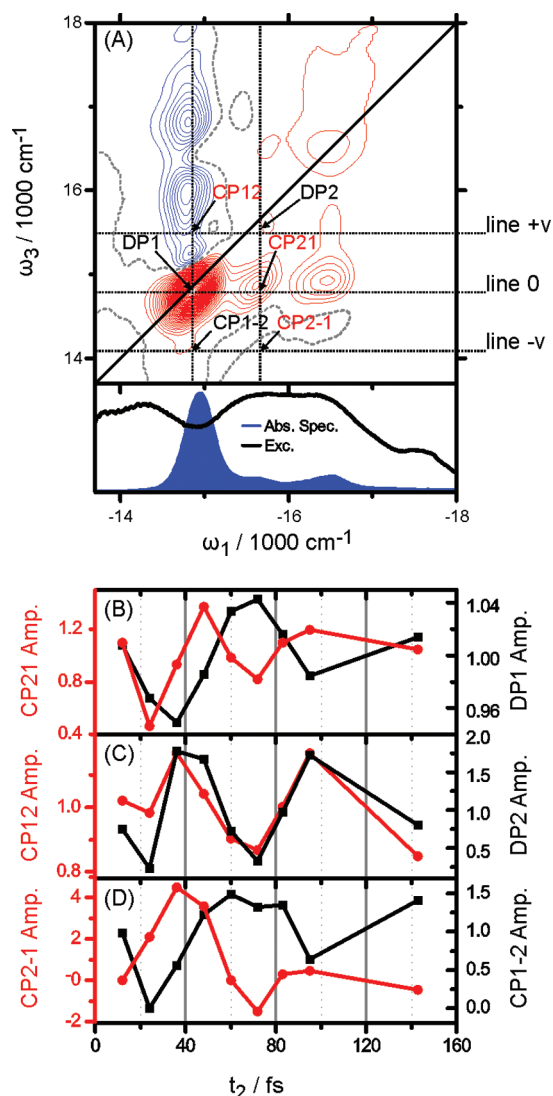
Figure 1. (A) Real part of the 2D-spectrum of ZnPc at $t_2 = 143$ fs. Red (blue) contour lines represent positive (negative) signals and are drawn in 2% steps, starting at 4%. The gray dashed line marks the nodal line at zero intensity. The signals along the diagonal line (black line at $\omega_1 = \omega_3$) correspond to peaks in the absorption spectrum (Abs. Spec.) as shown below in comparison to the excitation spectrum (Exc.). The horizontal dotted lines marked line 0 and $\pm$v are discussed in the text. (B−D) Dynamics of peaks indicated in panel A along t_2.
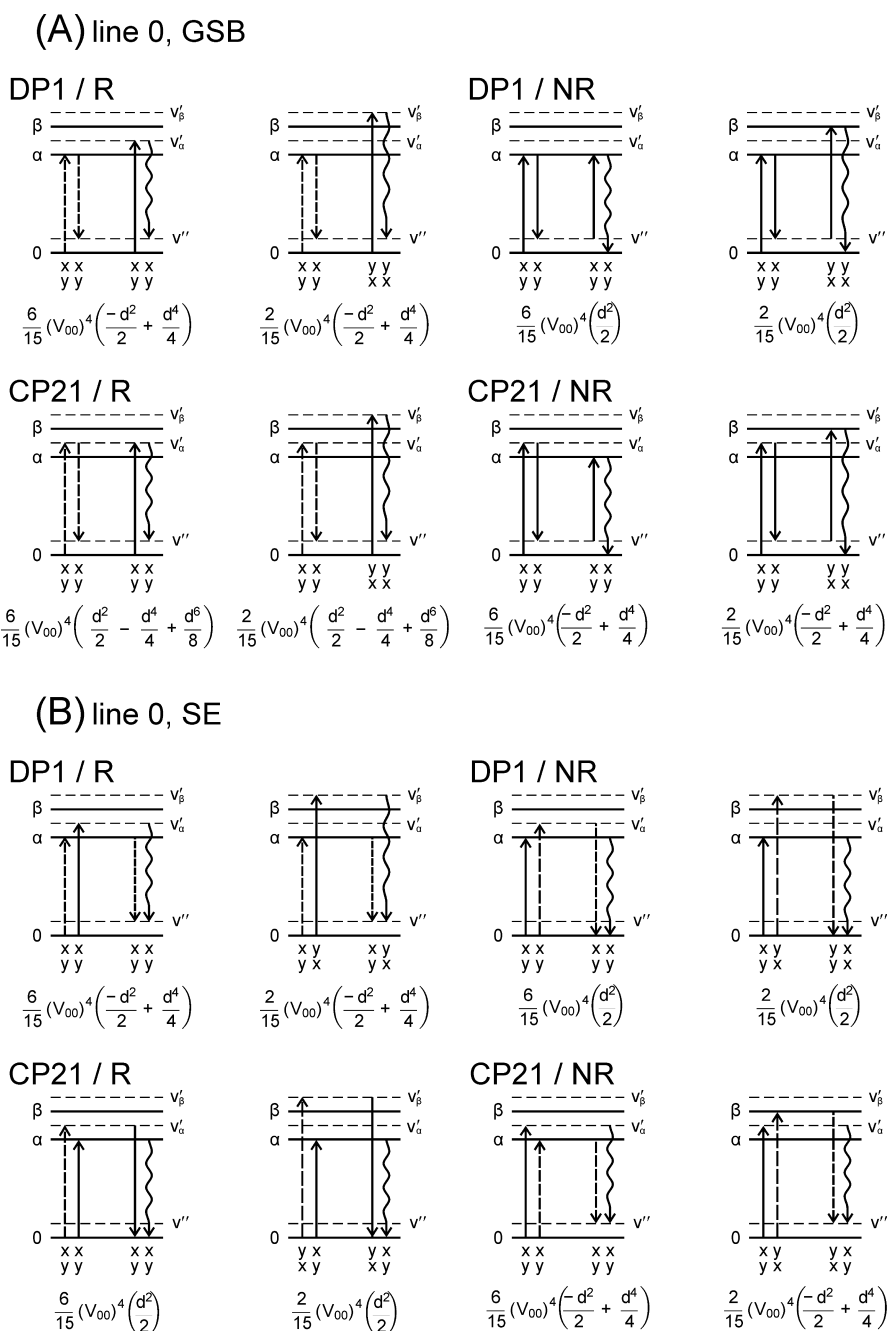
Figure 2. Energy ladder diagrams for oscillatory terms in GSB (A) and SE (B) for signals in level 0, divided into rephasing (R) and nonrephasing (NR) pathways. Electronic (vibrational) levels are depicted as horizontal full (dashed) lines. Bra-side and ket-side interactions and the resulting signal are shown as dashed, full, and wavy arrows, respectively. The orientation of the transition dipole moment in the molecular frame (e.g., xxyy) is shown underneath each interaction, followed by the product of the orientational average prefactor (e.g., 6/15) and the zero-phonon Franck–Condon factor, e.g., $V_{00} = \exp(-d^2/4)$.

system with the field and the emitted signal, respectively. Letters (x or y) underneath each interaction represent transition dipole moment unit vectors in the molecular frame. Given the low (TD)-B3LYP/SV(P) Huang−Rhys factor of the 700 cm^{-1} mode, we only include one vibrational level on each electronic state. The terms in front of the brackets are obtained by computing the orientationally averaged product of the transition dipole moments. Here, the ground and excited states are treated as harmonic potentials shifted with respect to each other by displacement d. The transition dipole moment

product can then be expressed via the Franck−Condon overlap integrals and the zero-phonon term $V_{00} = \exp(-d^2/4)$.

Each diagram in Figures 2 and 3 corresponds to a contribution modulating the 2D-spectrum as a function of t_2. Figure 2 summarizes the diagrams for line 0 (see Figure 1A), while Figure 3 shows the diagrams for lines +v and −v. The sign for each diagram is physically relevant, defining the phase of the oscillation. In this model, the sign can take the values +1 or −1, implying that oscillations are either in-phase or out-of-phase. To account for the oscillations in Figure 1B−D, one needs to sum up the oscillating pathways associated with each
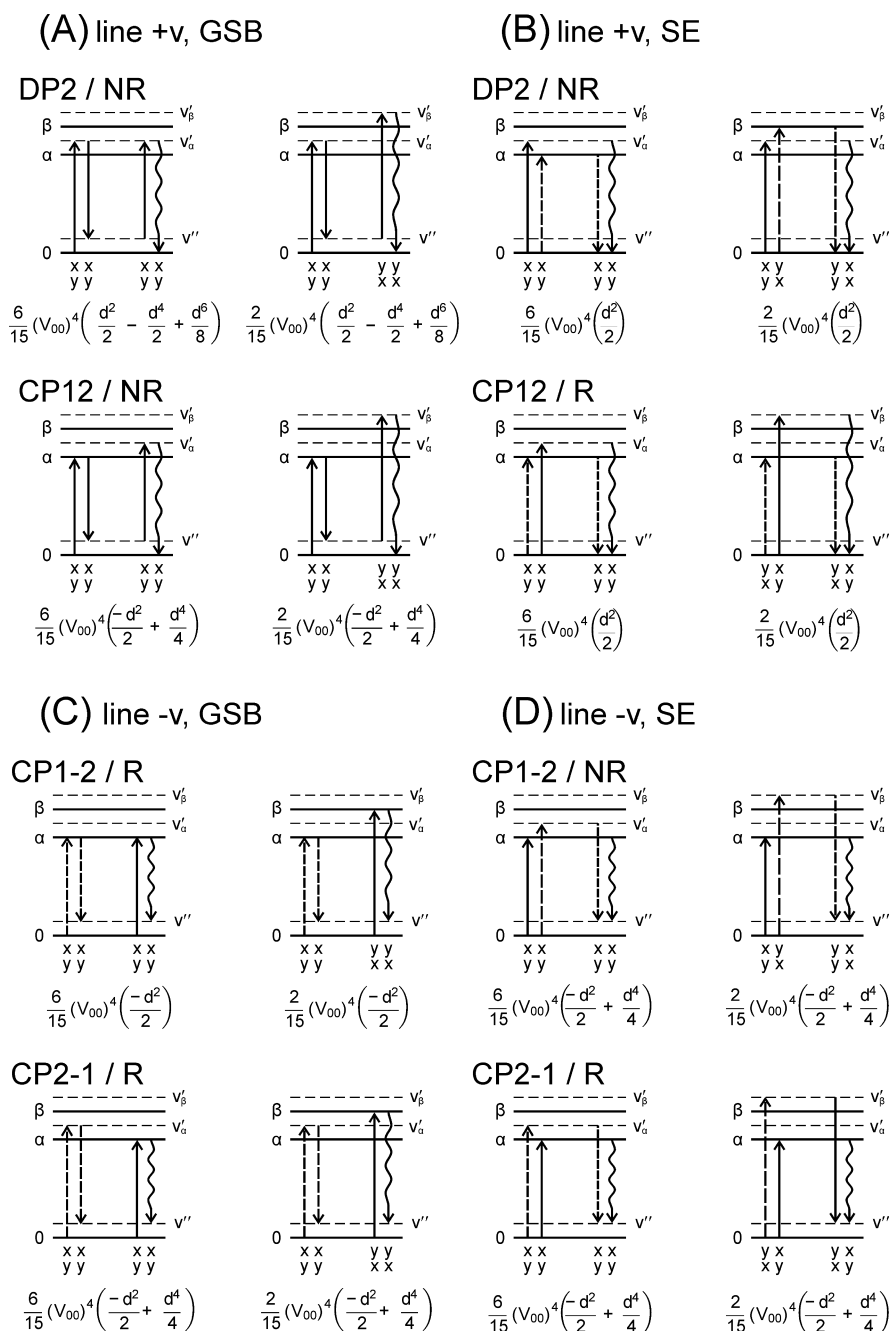
1499

dx.doi.org/10.1021/jz300362k | J. Phys. Chem. Lett. 2012, 3, 1497−1502

(A) line +v, GSB

DP2 / NR

$$\frac{6}{15}(V_{00})^4\left(\frac{d^2}{2} - \frac{d^4}{2} + \frac{d^6}{8}\right) \qquad \frac{2}{15}(V_{00})^4\left(\frac{d^2}{2} - \frac{d^4}{2} + \frac{d^6}{8}\right)$$

CP12 / NR

$$\frac{6}{15}(V_{00})^4\left(\frac{-d^2}{2} + \frac{d^4}{4}\right) \qquad \frac{2}{15}(V_{00})^4\left(\frac{-d^2}{2} + \frac{d^4}{4}\right)$$

(B) line +v, SE

DP2 / NR

$$\frac{6}{15}(V_{00})^4\left(\frac{d^2}{2}\right) \qquad \frac{2}{15}(V_{00})^4\left(\frac{d^2}{2}\right)$$

CP12 / R

$$\frac{6}{15}(V_{00})^4\left(\frac{d^2}{2}\right) \qquad \frac{2}{15}(V_{00})^4\left(\frac{d^2}{2}\right)$$

(C) line -v, GSB

CP1-2 / R

$$\frac{6}{15}(V_{00})^4\left(\frac{-d^2}{2}\right) \qquad \frac{2}{15}(V_{00})^4\left(\frac{-d^2}{2}\right)$$

CP2-1 / R

$$\frac{6}{15}(V_{00})^4\left(\frac{-d^2}{2} + \frac{d^4}{4}\right) \qquad \frac{2}{15}(V_{00})^4\left(\frac{-d^2}{2} + \frac{d^4}{4}\right)$$

(D) line -v, SE

CP1-2 / NR

$$\frac{6}{15}(V_{00})^4\left(\frac{-d^2}{2} + \frac{d^4}{4}\right) \qquad \frac{2}{15}(V_{00})^4\left(\frac{-d^2}{2} + \frac{d^4}{4}\right)$$

CP2-1 / R

$$\frac{6}{15}(V_{00})^4\left(\frac{-d^2}{2} + \frac{d^4}{4}\right) \qquad \frac{2}{15}(V_{00})^4\left(\frac{-d^2}{2} + \frac{d^4}{4}\right)$$

Figure 3. Energy ladder diagrams for oscillatory terms in lines +v and −v. The nomenclature is the same as that in Figure 2.

Table 1. Leading Terms in FC Factors for SE and GSB Pathways[a]

	$\omega_1(\text{DP1})$	$\omega_1(\text{CP21})$	sum
line +v	$\frac{8}{15}(V_{00})^4(1 - k)\frac{d^2}{2}$	$\frac{16}{15}(V_{00})^4 k\frac{d^2}{2}$	$\frac{8}{15}(V_{00})^4(1 + k)\frac{d^2}{2}$
line 0	$\frac{16}{15}(V_{00})^4(k - 1)\frac{d^2}{2}$	$-\frac{16}{15}(V_{00})^4(k - 1)\frac{d^2}{2}$	$\frac{16}{15}(V_{00})^4 k\frac{d^4}{4}$
line −v	$\frac{8}{15}(V_{00})^4(1 - k)\frac{d^2}{2}$	$-\frac{16}{15}(V_{00})^4 k\frac{d^2}{2}$	$-\frac{8}{15}(V_{00})^4(1 + k)\frac{d^2}{2}$

[a] k is the ratio of non-rephasing and rephasing contributions (NR/R), d is the zero-point displacement between the ground and first excited state, and $V_{00} = \exp(-d^2/4)$.

peak. The relative amplitude of nonrephasing and rephasing contributions, k, is found to be around 0.4 at all measured t_2 times. We describe the influence of k on the relative phase of the observed peaks in the Supporting Information. Table 1

1500

dx.doi.org/10.1021/jz300362k | J. Phys. Chem. Lett. 2012, 3, 1497−1502

summarizes the amplitudes of the oscillating contributions for the different peaks in the 2D spectrum. The columns show the expressions for different excitation frequencies ω_1 (DP1, CP21), and their sum, and the rows compare different lines in ω_3 (line 0, ± v).

We illustrate the results by a detailed discussion of the expressions for line 0. For DP1 and CP21, the leading amplitude terms have opposite sign. Therefore, the basic diagrammatic treatment of wavepackets[18−21] fully explains the out-of-phase oscillatory behavior of the 2D signals shown in Figure 1B. In pump-frequency-integrated techniques such as pump−probe or transient grating, DP1 and CP21 cannot be resolved in ω_1, meaning that the amplitude terms are summed up as expressed in the third column of Table 1. This leads to destructive interference of the oscillatory signal down to d^4, while the resolved signals in 2D-ES scale with the much more favorable d^2. Detection in lines +v or −v is advantageous for excitation-frequency-integrated techniques because there is no or only partial cancelation for these detection frequencies. We note, however, that 2D-ES offers an advantage for distinguishing vibrational coherences in ground and excited states, a long-standing problem in pump−probe.[22,23] Figure 3 shows that the rephasing signal near CP12 (CP12/R) is determined by excited state coherences, while CP12/NR will only show contributions from the electronic ground state. The opposite relation can be found for CP1−2.

The discussion of oscillatory patterns in 2D spectra is not limited to square-symmetric systems. The D_{4h} symmetry of ZnPc merely defines the orientational prefactor (e.g., 2/15 in Figures 2 and 3), and the same results (up to a constant) are obtained for nondegenerate first excited states. The vibrational wavepacket dynamics observed here are thus of general nature.

Distinguishing Electronic and Vibrational Coherence. For the comparison of electronic and vibrational coherence, it is interesting to identify the oscillating pathways that would occur in the purely "electronic" case. The diagrams in Figure 2 illustrate the argument for the distinction between electronic and vibrational coherences first made by Fleming and co-workers.[4,6] In the electronic dimer, there will be no contribution from pathways including ν'', leaving only SE-pathways DP1/NR and CP21/R in Figure 2. Hence, the electronic coherences will manifest as oscillations of the diagonal peaks in nonrephasing spectra and of cross-peaks in rephasing spectra, while in the vibrational system, all peaks will oscillate. In this case, the features in line −v depicted in Figure 3 are a unique vibrational signature.[7,24] The difference between electronic and vibrational coherence can therefore be reduced to the question of detecting an additional ground state level, which can only have vibrational origin. We note that the presence of an oscillatory signal in line −v distinguishes electronic and vibrational coherences without the need to dissect the signal into rephasing and nonrephasing contributions,[3,6] which is problematic for finite-duration-excitation pulses.

In a realistic molecular aggregate, both vibrational and electronic DOFs are present simultaneously. In this case, the resonance coupling between the pigments also acts on the vibrational DOFs, which leads to excited states with a mixed electronic-vibrational character (vibronic exciton states).[8] Analysis based on the arguments from the preceding paragraph would conclude that all coherences in this system are of electronic origin. However, some coherences will be largely vibrational in nature, enabling long coherence lifetimes.[10]

Furthermore, the frequencies of the vibronic exciton coherences are shifted from those of the vibrational modes, and a comparison with known ground-state frequencies would not unveil their largely vibrational origin.

Recent experiments[25] on the Fenna−Matthews−Olson complex (FMO) have shown oscillations on the diagonal in rephasing 2D spectra. On the basis of the arguments by Cheng and Fleming,[6] such oscillations would indicate vibrational origin. However, an additional observation by Panitchayang-koon et al.[25] is a 90° phase shift between the oscillations on the diagonal in the rephasing spectra and the corresponding oscillations of the crosspeak. Within the theory used in this work, this behavior cannot be explained as either electronic or vibrational coherences, as an analysis of the diagrams in Figures 2 and 3 only allows for 0 or 180° phase shifts. To explain the observed 90° phase shift, Panitchayangkoon et al.[25] invoked coherence-to-population transfer. When such nonsecular effects are included in the exciton model, all peaks in the 2D spectrum will oscillate. Coherence-to-population transfer is not allowed by the second-order quantum master equation for a vibrational mode weakly linearly coupled to the bath.[26] This excludes pure vibrational wavepackets as the origin of the long-lived oscillations in the 2D spectra of FMO. We note that nonsecular terms are, in general, nonzero for vibronic excitons, and the observation of such effects cannot be taken as a definite signature of purely electronic coherence.

From the discussion above, it is clear that a separation of electronic and nuclear coherences in a (realistic) molecular aggregate based on the experimental data alone is questionable. On the basis of a molecular aggregate's Raman spectra and excitonic structures, it is experimentally more feasible to distinguish coherences evolving in ground or excited states. Our contribution to this discussion is that an unambiguous sign for the involvement of a vibrational level on the ground state are signals on line −v. If such signals cannot be detected despite sufficient bandwidth, and the oscillations observed in lines 0 or +v do not correspond to known ground-state modes, then the coherences can be assigned to the excited state. As discussed above, this does not imply that the coherences are purely electronic in nature, because vibronic exciton coherences will oscillate with frequencies different from those of the vibrational mode. In this case, the dephasing time of the coherences could provide important information on the relative contribution of vibrational and electronic DOFs.

■ ASSOCIATED CONTENT

Ⓢ Supporting Information

We describe calibration procedures for time and frequency axes as well as the influence of $k = NR/R$ on the relative phase of the observed peaks. This information is available free of charge via the Internet at http://pubs.acs.org/.

■ AUTHOR INFORMATION

Corresponding Author

*E-mail: juergen.hauer@univie.ac.at.

Notes

The authors declare no competing financial interest.

■ ACKNOWLEDGMENTS

■ REFERENCES

(1) Mancal, T.; Bixner, O.; Christensson, N.; Hauer, J.; Milota, F.; Nemeth, A.; Sperling, J.; Kauffmann, H. F. Dynamics of Quantum Wave Packets in Complex Molecules Traced by 2D Coherent Electronic Correlation Spectroscopy. *Procedia Chem* **2011**, *3*, 105–117.

(2) Christensson, N.; Milota, F.; Hauer, J.; Sperling, J.; Bixner, O.; Nemeth, A.; Kauffmann, H. F. High Frequency Vibrational Modulations in Two-Dimensional Electronic Spectra and Their Resemblance to Electronic Coherence Signatures. *J. Phys. Chem. B* **2011**, *115*, 5383–5391.

(3) Turner, D. B.; Wilk, K. E.; Curmi, P. M. G.; Scholes, G. D. Comparison of Electronic and Vibrational Coherence Measured by Two-Dimensional Electronic Spectroscopy. *J. Phys. Chem. Lett.* **2011**, *2*, 1904–1911.

(4) Engel, G. S.; Calhoun, T. R.; Read, E. L.; Ahn, T. K.; Mancal, T.; Cheng, Y. C.; Blankenship, R. E.; Fleming, G. R. Evidence for Wavelike Energy Transfer through Quantum Coherence in Photosynthetic Systems. *Nature* **2007**, *446*, 782–786.

(5) Schlau-Cohen, G. S.; Ishizaki, A.; Fleming, G. R. Two-Dimensional Electronic Spectroscopy and Photosynthesis: Fundamentals and Applications to Photosynthetic Light-Harvesting. *Chem. Phys.* **2011**, *386*, 1–22.

(6) Cheng, Y. C.; Fleming, G. R. Coherence Quantum Beats in Two-Dimensional Electronic Spectroscopy. *J. Phys. Chem. A* **2008**, *112*, 4254–4260.

(7) Turner, D. B.; Dinshaw, R.; Lee, K.-K.; Belsley, M. S.; Wilk, K. E.; Curmi, P. M. G.; Scholes, G. D. Quantitative Investigations of Quantum Coherence for a Light-Harvesting Protein at Conditions Simulating Photosynthesis. *Phys. Chem. Chem. Phys.* **2012**, *14*, 4857–4874.

(8) Philpott, M. R. Theory of Coupling of Electronic and Vibrational Excitations in Molecular Crystals and Helical Polymers. *J. Chem. Phys.* **1971**, *55*, 2039–&.

(9) Womick, J. M.; Moran, A. M. Vibronic Enhancement of Exciton Sizes and Energy Transport in Photosynthetic Complexes. *J. Phys. Chem. B* **2011**, *115*, 1347–1356.

(10) Christensson, N.; Kauffmann, H. F.; Pullerits, T.; Mancal, T. Origin of Long Lived Coherences in Light-Harvesting Complexes. In *arXiv:1201.6325v1*, 2012.

(11) Nemeth, A.; Sperling, J.; Hauer, J.; Kauffmann, H. F.; Milota, F. Compact Phase-Stable Design for Single- and Double-Quantum Two-Dimensional Electronic Spectroscopy. *Opt. Lett.* **2009**, *34*, 3301–3303.

(12) Faeder, S. M. G.; Jonas, D. M. Two-Dimensional Electronic Correlation and Relaxation Spectra: Theory and Model Calculations. *J. Phys. Chem. A* **1999**, *103*, 10489–10505.

(13) Nemykin, V. N.; Hadt, R. G.; Belosludov, R. V.; Mizuseki, H.; Kawazoe, Y. Influence of Molecular Geometry, Exchange-Correlation Functional, and Solvent Effects in the Modeling of Vertical Excitation Energies in Phthalocyanines Using Time-Dependent Density Functional Theory (TDDFT) and Polarized Continuum Model TDDFT Methods: Can Modern Computational Chemistry Methods Explain Experimental Controversies? *J. Phys. Chem. A* **2007**, *111*, 12901–12913.

(14) Savolainen, J.; van der Linden, D.; Dijkhuizen, N.; Herek, J. L. Characterizing the Functional Dynamics of Zinc Phthalocyanine from Femtoseconds to Nanoseconds. *J. Photochem. Photobiol. A* **2008**, *196*, 99–105.

(15) Nemeth, A.; Milota, F.; Mancal, T.; Lukes, V.; Hauer, J.; Kauffmann, H. F.; Sperling, J. Vibrational Wave Packet Induced Oscillations in Two-Dimensional Electronic Spectra. I. Experiments. *J. Chem. Phys.* **2010**, *132*, 184514.

(16) Mancal, T.; Nemeth, A.; Milota, F.; Lukes, V.; Kauffmann, H. F.; Sperling, J. Vibrational Wave Packet Induced Oscillations in Two-Dimensional Electronic Spectra. II. Theory. *J. Chem. Phys.* **2010**, *132*, 184515.

(17) Gierschner, J.; Mack, H. G.; Luer, L.; Oelkrug, D. Fluorescence and Absorption Spectra of Oligophenylenevinylenes: Vibronic Coupling, Band Shapes, and Solvatochromism. *J. Chem. Phys.* **2002**, *116*, 8596–8609.

(18) Farrow, D. A.; Smith, E. R.; Qian, W.; Jonas, D. M. The Polarization Anisotropy of Vibrational Quantum Beats in Resonant Pump−Probe Experiments: Diagrammatic Calculations for Square Symmetric Molecules. *J. Chem. Phys.* **2008**, *129*, 174509.

(19) Farrow, D. A.; Qian, W.; Smith, E. R.; Ferro, A. A.; Jonas, D. M. Polarized Pump−Probe Measurements of Electronic Motion via a Conical Intersection. *J. Chem. Phys.* **2008**, *128*, 144510.

(20) Qian, W.; Jonas, D. M. Role of Cyclic Sets of Transition Dipoles in the Pump−Probe Polarization Anisotropy: Application to Square Symmetric Molecules and Perpendicular Chromophore Pairs. *J. Chem. Phys.* **2003**, *119*, 1611–1622.

(21) Smith, E. R.; Farrow, D. A.; Jonas, D. M. Response Functions for Dimers and Square-Symmetric Molecules in Four-Wave-Mixing Experiments with Polarized Light. *J. Chem. Phys.* **2005**, *123*, 044102.

(22) Jonas, D. M.; Bradforth, S. E.; Passino, S. A.; Fleming, G. R. Femtosecond Wavepacket Spectroscopy - Influence of Temperature, Wavelength, and Pulse Duration. *J. Phys. Chem.* **1995**, *99*, 2594–2608.

(23) Kahan, A.; Nahmias, O.; Friedman, N.; Sheves, M.; Ruhman, S. Following Photoinduced Dynamics in Bacteriorhodopsin with 7-fs Impulsive Vibrational Spectroscopy. *J. Am. Chem. Soc.* **2007**, *129*, 537–546.

(24) Butkus, V.; Zigmantas, D.; Valkunas, L.; Abramavicius, D. Vibrational vs. Electronic Coherences in 2D Spectrum of Molecular Systems. In *arXiv:1201.2753v1*, 2012.

(25) Panitchayangkoon, G.; Voronine, D. V.; Abramavicius, D.; Caram, J. R.; Lewis, N. H. C.; Mukamel, S.; Engel, G. S. Direct Evidence of Quantum Transport in Photosynthetic Light-Harvesting Complexes. *Proc. Natl. Acad. Sci. U.S.A.* **2011**, *108*, 20908–20912.

(26) Mancal, T.; May, V. Non-Markovian Relaxation in an Open Quantum System - Polynomial Approach to the Solution of the Quantum Master Equation. *Eur. Phys. J. B* **2000**, *18*, 633–643.